ChemistrySelect

Research Article
doi.org/10.1002/slct.202201793

Chemistry Europe
European Chemical Societies Publishing

www.chemistryselect.org

Designing of Thiazolidinones for COVID-19 and its Allied Diseases: An *In silico* Evaluation

Muhammad Asam Raza,*[a] Umme Farwa,[a] Nida Qurat Ul Ain,[a] Fatima Ishaque,[a] Muhammad Yaseen,[b] Muhammad Naveed,[c] and Muhammad Aqib Shabbir[c]

In silico studies in terms of density functional theory (DFT), molecular docking, and ADMET (absorption, distribution, metabolism, excretion and toxicity) were performed for 55 thiazolidinones compounds derived from different amines and aldehydes. DFT is a computational quantum mechanical modeling method used to predict the various properties of the compounds. Different parameters such as Electronegativity (x), Chemical Hardness (η), Chemical Potential (μ), Ionization potential (IP), and Electron Affinity (EA), etc. were calculated by Koopmans theorem. The compounds were docked with Molecular Operating Environment (MOE) software using already reported PDB files of BChE, AChE, and α-glucosidase. To analyze the Spike Glycoprotein of SARS-Cov-2 and heterocyclic compounds, molecular interactions study was carried out between Spike Glycoprotein of SARS-Cov-2 (6VXX) and 55 synthetic heterocyclic compounds. It was performed by the utilization of PyRx Virtual Screening Tool and AutoDock Vina based virtual environment was used in PyRx. Maximum binding affinity was observed with compound **A7** which was −8.7 kcal/mol and then with **A5** which was −8.5 respectively. In the case of the AChE enzyme, **B5** has a maximum docking score of −12.9027 kcal/mol while **C7** depicted the maximum score for the BChE enzyme with a value of −8.6971 kcal/mol. The docking studies revealed that **C6** compound has maximum binding capacity toward glucosidase (−14.8735 kcal/mol). ADMET properties of under consideration compounds were determined by Swiss online-based software which concluded that these molecules have a drug-like properties and having no violation.

Introduction

The word virus mainly derived from latin word "venom" means poison.[1] Corona viruses are encased positive-sense RNA viruses 60–140 nm in diameter with superficially spike-like projections that gives it a crown-like expression beneath the electron microscope; henceforth the name coronavirus.[2] World Health Organization declared coronavirus-2019 as COVID-2019, a pandemic disease that is why it is a very serious concern for us.[3] The severe acute respiratory syndrome corona virus 2[4] is fast spreading from its origin in Wuhan City of Hubei Province of China to all over the world.[5] The primary lethal case was testified on 11th Jan 2020 and huge relocation of Chinese throughout the Chinese New Year fueled the prevalent. A number of cases in other domains of China and other countries were reported in public those were coming back from Wuhan. Four corona viruses namely NL63, HKU1, OC43, and 229E have been in flow in humans, and normally cause slight respiratory disease.[6]

COVID virus caused the serve acute respiratory syndrome[4] in humans.[7] It is considered that the COVID virus transferred from the bat to animals and then moved in humans.[3] Infection is spread by large droplets produced in coughing and sneezing, by inhalation of these droplets or touching the eyes, nose, and mouth after touching the contaminated surface. The presence of the virus is also in the stool and adulteration of the water supply and following spread via aerosolization and the oral route is also observed.[8,9] When COVID enters the central nervous system (CNS) by different routes like infected lymphocytes, olfactory neutron, etc., it distributes in the blood-brain barrier (BBB).[10,11] In old age people, there is more chance to enter the CNS.[12] The person with diabetes also has a greater risk of both nerve and infection of COVID-17.[13,14] Type 1 diabetics person have greater risk as compared to diabetics 2 because in first one glucose value is close to the target of developing COVID-19.[15] Studies have revealed higher viral lots in the nasal passage as compared to the throat with no change in viral burden among symptomatic and asymptomatic people.[16] The symptoms of fever (not in all), sore throat, cough, headache, fatigue, myalgia, and breathlessness were seen.[17] In the world, almost 1,192,028 cases are reported and about 64,316 deaths occurred till 4th April 2021.[18]

Many researchers are continuously working on the development of drugs and medicine for the treatment of this pandemic situation. They have worked on complex protease SARS-CoV-2 with PDB 1D: 6LU7 after confirming its three-dimensional crystal structure.[4,19,20] Heterocyclic compounds comprise the basic structural unit associated with the chief marketed drugs.[21] A database study of U.S.FDA-approved drugs was accomplished and it disclosed that 59% of small molecular drugs contain nitrogen in heterocyclic rings.[22] In the last

[a] *Dr. M. A. Raza, U. Farwa, N. Q. U. Ain, F. Ishaque*
Department of Chemistry, Hafiz Hayat Campus,
University of Gujrat, Gujrat, Pakistan
E-mail: asamgcu@yahoo.com
[b] *Dr. M. Yaseen*
Department of Chemistry, Division of Science and Technology,
University of Education, Lahore, Pakistan
[c] *Dr. M. Naveed, M. A. Shabbir*
Department of Biotechnology, University of Central Punjab,
Lahore, Pakistan

decade, many types of thaizolidinone derivatives was produced for pharmaceutical purposes. The five-member ring containing sulfur such as thaizolidinone compounds are mostly used for biological activities.[23] It is a heterocyclic compound comprising nitrogen, oxygen, and sulfur which is produced by oxo derivatization of thiazolidine.[24]

Thaizolidinone derivatives have vital biological activities in the recent era for example in antimicrobial,[25] antioxidants, analgesic,[23] peroxisome proliferator activator gamma receptor (PPAR), antitumor, cystic fibrosis transmembrane conductance regulator (CFTR), anti-diabetics,[26] anti-inflammatory, and agonist for follicle-stimulating hormone (FSH).[24,27]

An accurate method for treatment of COVID-19 is not available at this time so researchers are being used the previous antiviral drugs for the COVID-19 as the best strategy for treatment.[28] Most competent docking tools must be capable to envisage appropriately the ligand position within the binding site of the receptor and also give data about the molecular interactions linked with it.[29] Several compounds are screened as inhibitory effects of COVID-19 through in-silico studies. Keeping in view the importance of COVID-19 toward the health problems of human beings, the present project was designed to check the potential of synthesized and proposed thiazolidinones against COVID-19, Alzheimer and Diabetic using in-silico models.

Methods and Materials

Ligand Preparation

The synthesis of **D** and **E** series molecules was carried out according to already reported three-step methods of our research group.[30–33] The synthesis of the compounds (**E2**, **E4**, **E6**, **E7**, and **E8**) was done by condensing **E** with different aldehydes and already reported methods.[33] The synthesis of the remaining compounds (**A**, **B**, and **C** series) was proposed according to the above-mentioned protocols. The precursors (**A**–**C**) were designed via three steps method which further reacts with various aldehydes to convert into their respective compounds as mentioned in the synthetic scheme 1.

Density Functional Theory

The quantum chemical calculations were performed with Gaussian 09 and results were seen with the help of Gauss View 5.0.[34] The 6-31G (d, p) basis set and hybrid functional B3LYP method were used to optimize the geometry of compounds without symmetry resistance.[35,36] Polarized function on all atoms was chosen with the helped of 6-31 G (d, p) basis set. In order to determine the structure as true minima then frequency calculations were also performed.[33,36–38]

Docking studies

A Molecular Operating Environment (MOE) software was used to perform docking experiments. Acetylcholinesterase, butyrylcholinesterase, and alpha-glucosidase of crystal structure were selected for studies with their PDB codes 1EVE, 4BDS, and 2Q85 respectively. In protein structure, all water molecules were removed, and then added hydrogen atoms. The default force field process was used for the optimization of energy while three-dimension protonation and energy minimization were carried with the help of the default parameter of the MOE energy minimization algorithm of downloaded enzymes. Enzyme active site was determined with the help of residue of reference ligand within 10 A° in the case of 1EVE[39] while 1POI (BChE) and α-glucosidase dummy atoms and active sites of the enzymes were determined using the alpha sphere. 2D ligand enzyme interaction was checked with the help of the ligand interaction module of MOE. Docking results and analysis with graphical representation were determined with the help of MOE and the discovery studio visualizer.[33,40] For interactional analysis of Spike Glycoprotein of SARS-Cov2 and 55 heterocyclic compounds, The protein was retrieved from the Protein Data Bank from the PDB ID of 6VXX. The synthetic heterocyclic compunds were converted into PDB format from conical SMILES by utilization of OpenBable. All the compounds were served as ligands and their energy was minimized before proceeding. PyRx Virtual Screening Tool was used for the docking analysis and the interactions were characterized on the basis of binding affinities in kcal/mol.[41]

Normal Mode Analysis The iModS online tool (http://imods.chaconlab.org/) was used to conduct the Normal Mode Analysis.[42] It is based on an examination of the complex's torsional angles. Examine the RMSD values, covariance among individual residues, eigon value of interacting residues, and structural deformation. It determines the complex's stability based on detailed coordinates study.

ADMET

In-silico ADMET study was used to measure various physiochemical and pharmacokinetic parameters of the designed compounds. For the drug discovery and research of unsafe chemical substances, the evaluation of the ADMET profile for drug moieties and environmental chemical substances had been important. Drug-like characteristics were studied as solubility, *pKa*, lipophilicity, absorption, permeability, bioavailability, blood-brain-barrier (BBB), penetration, metabolism, plasma-protein binding, drug-drug interaction, metabolism, synthetic accessibility, and molecular weight. ADMET estimation of thiazolidinones was done by Swiss online software http://www.swissadme.ch/.[43,44]

Results and Discussion

Our research group is continuously engaged in designing and synthesizing new compounds which may be used as inhibitors against different ailments. The current project is part of our work to synthesize/design a new potent molecule having a good effect on various clinical-related enzymes for human beings. The 55 compounds belong from 5 series (**A--E**) were selected for studies and among these compounds, **D**, **E**, **E2**, **E4**, **E6**, **E7**, and **E8** were already reported by our research group

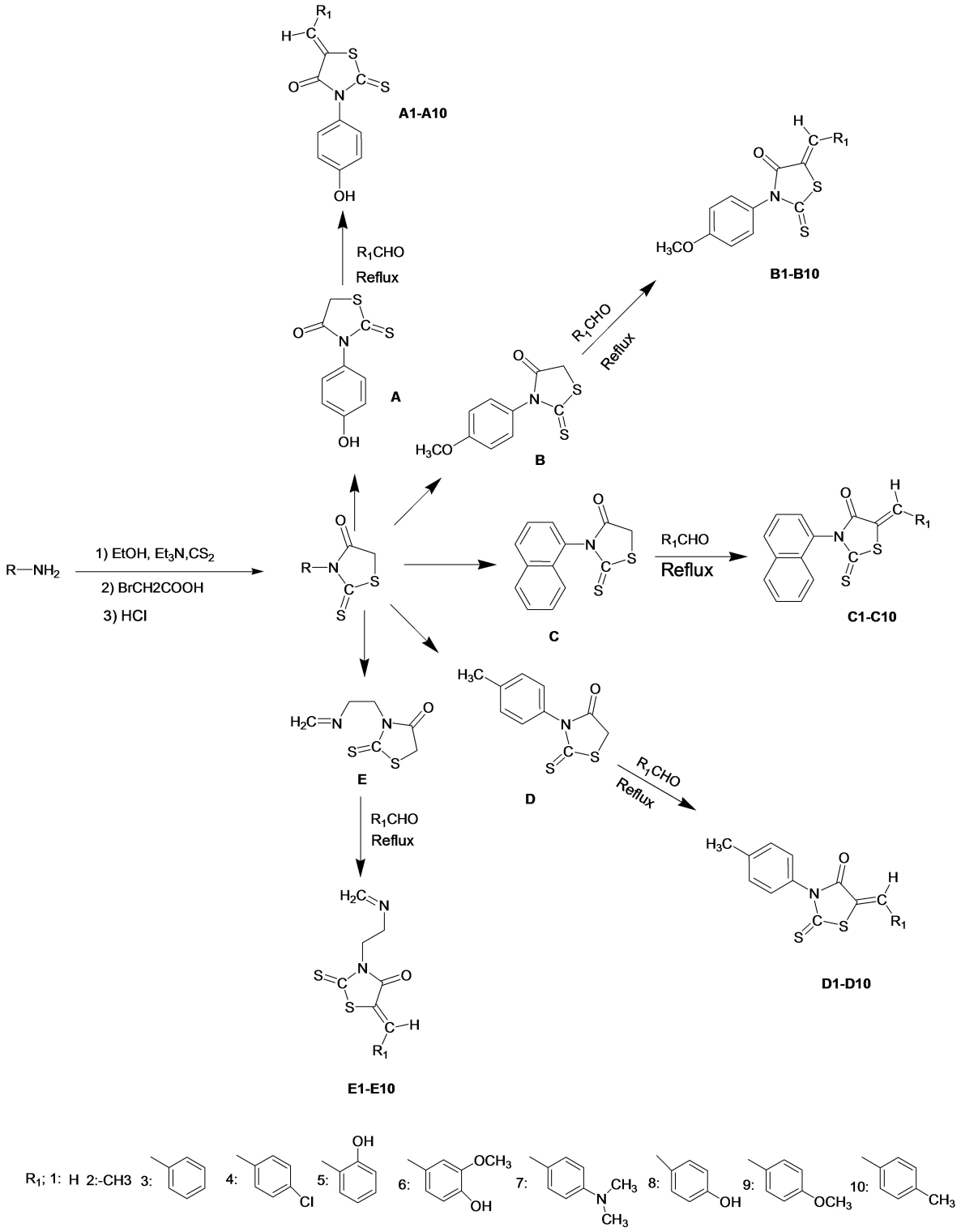

Scheme 1. The synthetic scheme for the synthesized and proposed compounds.

while the remaining compounds were proposed as they have a similar skeleton which already reported.

Density Functional Theory

The determination of the electronic properties of the molecules or atoms, density functional theory (DFT) is being used throughout the world.[45] It is a computational quantum

mechanical modeling method used to predict the various properties of the compounds. The structure of different inhibitors was proposed and optimized with the help of the DFT methods. Different parameters such as Electronegativity (x), Chemical Hardness (η), Chemical Potential (μ), Ionization potential (IP), and Electron Affinity (EA), etc. were calculated and given in Tables 1,2,3. However, the optimized structure of compounds were represented in Figure 1. The Lowest Unoccupied Molecular Orbitals (LUMO) and the Highest Occupied Molecular Orbitals (HOMO) are called as frontier molecular orbital. LUMO has the capacity to accept an electron so it is an electron acceptor whereas HOMO has the ability to donate an electron so it is called an electron donor. Electron density localization of molecular orbital are determined with the help of FMO.[46,47] The electron-donating and electron-accepting properties of the molecule also determined by HOMO and LUMO. The energy gap diagram was represented in Figure 2. HOMO and LUMO energy gaps also helped to calculate the charger interaction within the molecules.

It was found on the basis of results that **B7** compound depicted highest HOMO energy (-0.19696) among all the series. For very first series of 4-Aminophenol the decreasing order of HOMO is **A7** > **A6** > **A9** > **A8** > **A5** > **A10** > **A3** > **A2** > **A4** > **A1** > **A** and for the second series of 4-methoxybenzeneamine, the order is **B7** > **B6** > **B9** > **B5** > **B8** > **B10** > **B3** > **B2** > **B1** > **B4** > **B** and the C series compound the order of HOMO is **C7** > **C6** > **C9** > **C5** > **C8** > **C10** > **C3** > **C2** > **C4** > **C1** > **C**. The LUMO order is **A7** > **A2** > **A9** > **A5** > **A8** > **A10** > **A6** > **A1** > **A3** > **A4** and for the second series, the order is **B3** > **B7** > **B2** > **B9** > **B5** > **B8** > **B10** > **B6** > **B1** > **B4** > **B** and the C series compound the order of LUMO is **C7** > **C2** > **C9** > **C6** > **C5** > **C8** > **C10** > **C1** > **C3** > **C4** > **C**.

For all series of **A**, **B**, and **C** when no substitution is present on the thaizolidinone ring the value of HOMO and LUMO is minimum. But when very strong -I (inductive) group 4-dimethlaminobenzledyhe present on all series of compounds then value increase both for HOMO and LUMO. The presence of weak -I group for example, formaldehyde, acetaldehyde and benzaldehyde then its value lowers as in **A** compound series however, when there are strong -I group, for example, 2-

Table 1. HOMO, LUMO, and Electrochemical properties of the hypothetical **A** series compounds.

Properties	A	A1	A2	A3	A4	A5	A6	A7	A8	A9	A10
μ (chemical potential)	−0.21786	−0.16517	−0.15902	−0.16317	−0.16932	−0.15877	−0.15691	−0.14071	−0.15854	−0.15648	−0.16055
η (chemical hardness)	−0.04906	−0.06748	−0.06908	−0.06407	−0.06298	−0.06388	−0.06068	−0.05719	−0.06349	−0.06282	−0.06434
1/2η (chemical Softness)	−10.1916	−7.41015	−7.23851	−7.80457	−7.93903	−7.82779	−8.24063	−8.74279	−7.87588	−7.95925	−7.77182
X (electronegativity)	0.21786	0.165165	0.159015	0.163165	0.16932	0.158765	0.156905	0.14071	0.158535	0.15648	0.160545
HOMO	−0.26692	−0.23264	−0.22809	−0.22723	−0.2323	−0.22264	−0.21758	−0.1979	−0.22202	−0.2193	−0.22488
LUMO	−0.1688	−0.09769	−0.08994	−0.0991	−0.10634	−0.09489	−0.09623	−0.08352	−0.09505	−0.09366	−0.09621
(LUMO-HOMO)	0.09812	0.13495	0.13815	0.12813	0.12596	0.12775	0.12135	0.11438	0.12697	0.12564	0.12867
Energy gap (eV)	0.003606	0.00496	0.005077	0.004709	0.00462	0.00469	0.00446	0.00420	0.00466	0.00461	0.00472
IP (ionization potential)	0.26692	0.23264	0.22809	0.22723	0.2323	0.22264	0.21758	0.1979	0.22202	0.2193	0.22488
EA (electron affinity)	0.1688	0.09769	0.08994	0.0991	0.10634	0.09489	0.09623	0.08352	0.09505	0.09366	0.09621
Electrophilicity index (ω)	−0.48372	−0.20215	−0.18303	−0.20778	−0.22761	−0.19731	−0.20288	−0.1731	−0.19795	−0.19489	−0.20032
Maximum charge transfer(△Nmax)	−4.44068	−2.4478	−2.30206	−2.54687	−2.68847	−2.48556	−2.58599	−2.4604	−2.4972	−2.49093	−2.49545

Table 2. HOMO, LUMO, and Electrochemical properties of the hypothetical **B** series compounds.

Properties	B	B1	B2	B3	B4	B5	B6	B7	B8	B9	B10
μ (chemical potential)	−0.2179	−0.16301	−0.15707	−0.1614	−0.16739	−0.15701	−0.15574	−0.13966	−0.15777	−0.15529	−0.15869
η (chemical hardness)	−0.049	−0.06683	−0.06861	−0.06377	−0.06247	−0.06337	−0.06078	−0.05731	−0.06342	−0.06284	−0.06373
1/2η (chemical Softness)	−10.204	−7.48167	−7.28757	−7.84068	−8.00384	−7.89079	−8.22639	−8.72524	−7.88457	−7.95672	−7.84621
X (electronegativity)	0.21791	0.16301	0.15707	0.1614	0.16739	0.157005	0.15574	0.13966	0.15776	0.1553	0.15868
HOMO	−0.2669	−0.22984	−0.22568	−0.22517	−0.22986	−0.22037	−0.21652	−0.19696	−0.22118	−0.2181	−0.22241
LUMO	−0.1689	−0.09618	−0.08846	0.09763	−0.10492	−0.09364	−0.09496	−0.08235	−0.09435	−0.0925	−0.09496
(LUMO-HOMO)	0.09800	0.13366	0.13722	0.12754	0.12494	0.12673	0.12156	0.11461	0.12683	0.1257	0.12745
Energy gap (eV)	0.00360	0.00491	0.00504	0.00469	0.00459	0.00466	0.00447	0.00421	0.00466	0.0046	0.00468
IP (ionization potential)	0.26691	0.22984	0.22568	0.22517	0.22986	0.22037	0.21652	0.19696	0.22118	0.21813	0.22241
EA (electron affinity)	0.16891	0.09618	0.08846	0.09763	0.10492	0.09364	0.09496	0.08235	0.09435	0.09245	0.09496
Electrophilicity index (ω)	−0.4845	−0.1988	−0.17979	−0.20425	−0.22426	−0.19451	−0.19953	−0.17017	−0.19625	−0.19188	−0.19757
Maximum charge transfer (△Nmax)	−4.4471	−2.43917	−2.28932	−2.53097	−2.67953	−2.47779	−2.56236	−2.43705	−2.48782	−2.4712	−2.49015

Table 3. HOMO, LUMO, and Electrochemical properties of the hypothetical **C** series compounds.

Properties	C	C1	C2	C3	C4	C5	C6	C7	C8	C9	C10
μ (chemical potential)	−0.23412	−0.16291	−0.15747	−0.16149	−0.16698	−0.15759	−0.15529	−0.1406	−0.15802	−0.15561	−0.1592
η (chemical hardness)	−0.03288	−0.06529	−0.06758	−0.06261	−0.06086	−0.06293	−0.06114	−0.05724	−0.06315	−0.06275	−0.06323
1/2η (chemical Softness)	−15.2068	−7.65873	−7.39864	−7.98594	−8.21558	−7.94597	−8.17862	−8.73591	−7.91828	−7.96876	−7.90764
X (electronegativity)	0.23412	0.162905	0.15747	0.16149	0.16698	0.157585	0.15528	0.14059	0.158015	0.155605	0.1592
HOMO	−0.267	−0.22819	−0.22505	−0.2241	−0.22784	−0.22051	−0.21642	−0.19783	−0.22116	−0.21835	−0.22243
LUMO	−0.20124	−0.09762	−0.08989	−0.09888	−0.10612	−0.09466	−0.09415	−0.08336	−0.09487	−0.09286	−0.09597
(LUMO-HOMO)	0.06576	0.13057	0.13516	0.12522	0.12172	0.12585	0.12227	0.11447	0.12629	0.12549	0.12646
Energy gap (eV)	0.002417	0.004799	0.004967	0.004602	0.004473	0.004625	0.00449	0.004207	0.004641	0.004612	0.00465
IP (ionization potential)	0.267	0.22819	0.22505	0.2241	0.22784	0.22051	0.21642	0.19783	0.22116	0.21835	0.22243
EA (electron affinity)	0.20124	0.09762	0.08989	0.09888	0.10612	0.09466	0.09415	0.08336	0.09487	0.09286	0.09597
Electrophilicity index (ω)	−0.83352	−0.20325	−0.18346	−0.20827	−0.22907	−0.19732	−0.19721	−0.17268	−0.19771	−0.19295	−0.20042
Maximum charge transfer (△Nmax)	−7.12044	−2.49529	−2.33013	−2.5793	−2.74367	−2.50433	−2.54003	−2.45645	−2.50242	−2.47996	−2.51779

hydroxybenzldehyde, 4-hydroxy-3-methoxy benzaldehyde, 4-hdroxbenzldehe and 4-methoxybenzldehe present then energy gap is increased.[43]

In **A** series compound phenol group is present and its value for HOMO and LUMO is less as compared to **B** and **C** series compounds because phenol has five resonating structures. In the **B** series, the methoxy group is present and its value high as compare to **A** series compounds because it has 4 resonating structures and in case of naphthalene three reasoning structures present so its value high as compare to **A** and **B** series compounds.[48,49]

Koopmans theorem was used to calculate the chemical potential (μ), electronegativity (x), and chemical hardness (η), and formulas were given below;

$$\text{Electronegativity } (x) = -[E_{HOMO} + E_{LUMO}]/2 \quad (1)$$

$$\text{Chemical Hardness } (\eta) = -[E_{LUMO} - E_{HOMO}]/2 \quad (2)$$

$$\text{Chemical Potential } (\mu) = [E_{HOMO} + E_{LUMO}]/2 \quad (3)$$

$$\text{Ionization potential } (IP) = -E_{HOMO} \quad (4)$$

$$\text{Electron Affinity } (EA) = -E_{LUMO} \quad (5)$$

The difference in HOMO and LUMO predicted the reactivity and chemical softness of compounds while electron affinity and ionization potential included in the global reactivity parameter was also determined with the help of these parameters. The energy gap between compounds predicts the chemical hardness and softness nature of the molecules. Larger the energy gap hardness of the behavior of the molecules and vice versa. Results were predicted that these compounds can be easily prepared in wet lab because these compounds have IP values for **A** series compounds are 0.1979, 0.21758, 0.2193, 0.22202, 0.22264, 0.22488, 0.22723, 0.22809, 0.2323, 0.23264, 0.26692 and **B** series compounds are 0.19696, 0.21652, 0.21813, 0.22037, 0.22118, 0.22241, 0.22517, 0.22568, 0.22984, 0.22986, 0.26691 and for **C** series compounds are 0.19783, 0.21642, 0.21835, 0.22051, 0.22116, 0.22243, 0.2241, 0.22505, 0.22784, 0.22819 and 0.267. IP values helped to predict the strength of the chemical bond and from all series, **A**, **B**, and **C** compounds and compound **C** has maximum IP value which was 0.267 so it may be more easily prepared in wet lab as compared to compound **B7** because it has lower IP value 0.19696. The use of global chemical potential parameter helped to calculate the chemical nature of compounds theoretically. Chemical potential of **A** series compounds ranged from −0.21786 to −0.14071 maximum μ was exhibited by **A7** while compound **A** has the least value and is similar **B** and **C** series compounds. Electron affinity has an important role to predict the chemical behavior of the compounds using the Koopmans theorem. Compound **C** has a maximum EA 0.20124 value in all series compound **A**, **B**, and **C** while compound **B7** has the least 0.08235. Different substitutions on the benzene ring showed variance on parameter. Methyl group has +I effect while OH, OCH_3, and Cl and $N(CH_3)$ have –I by attaching this different electron-withdrawing and electron-donating groups on the benzene ring showed a different effect on the parameters (x, η, μ, etc.). The EN value has increased from 0.157005 to 0.167398 when -I group is attached. Different effects at different positions of benzene ring especially at ortho and para positions showed more effect. Electronegativity enhances when an electron-withdrawing group is present and vice versa. Different types of physical and chemical properties were determined with the help of DFT calculation.[43,50]

Docking studies

Molecular docking is a structure-based virtual screening (SBVS) and is used to make the interactive computer-generated structures of the molecules with the selected target in multiple conformations, positions, and orientations.[43,51] It is very appreciated in the structure-based rational drug designing and

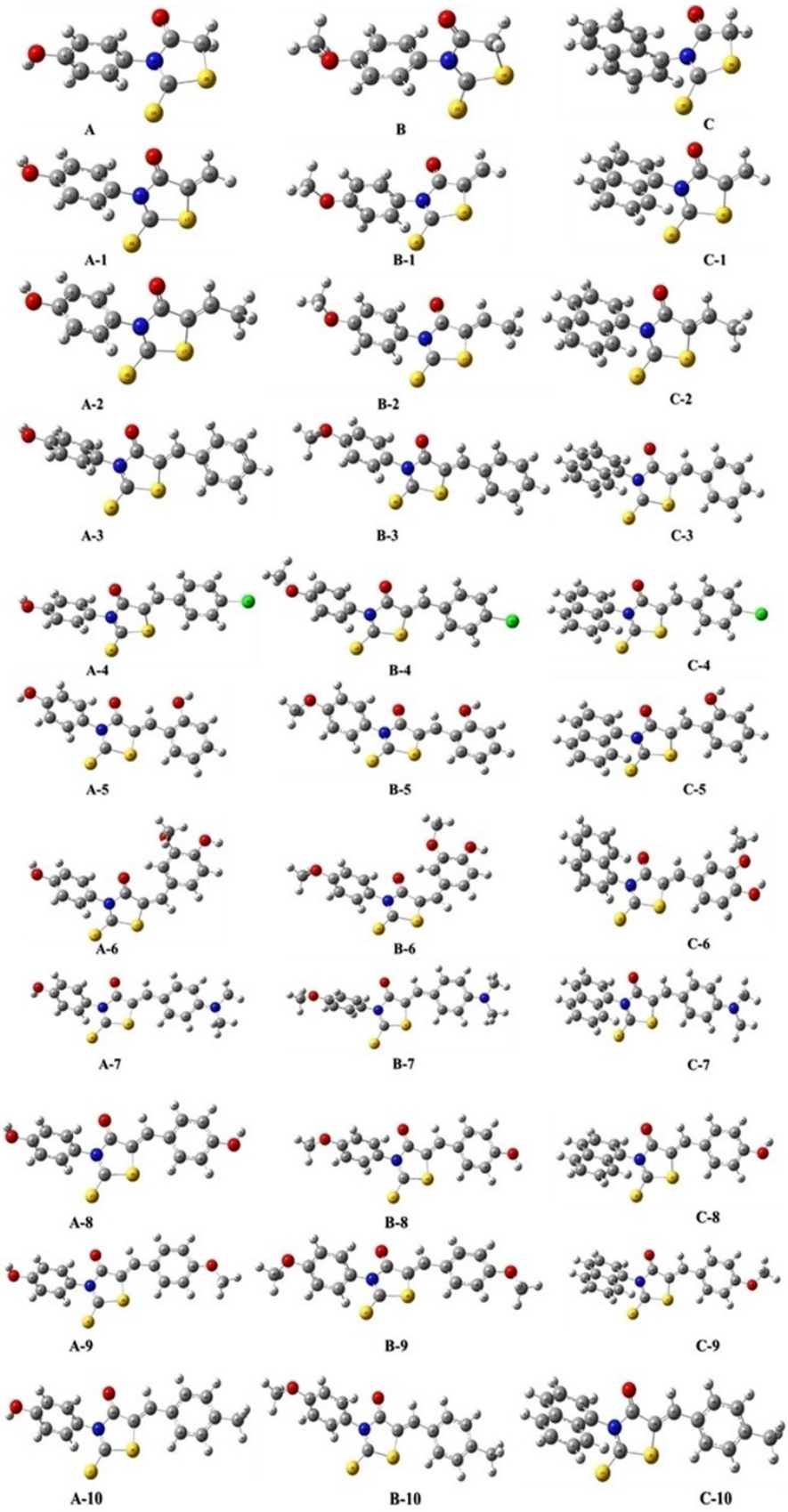

Figure 1. Optimized structures of the hypothetical compounds **A**, **B**, and **C** Series.

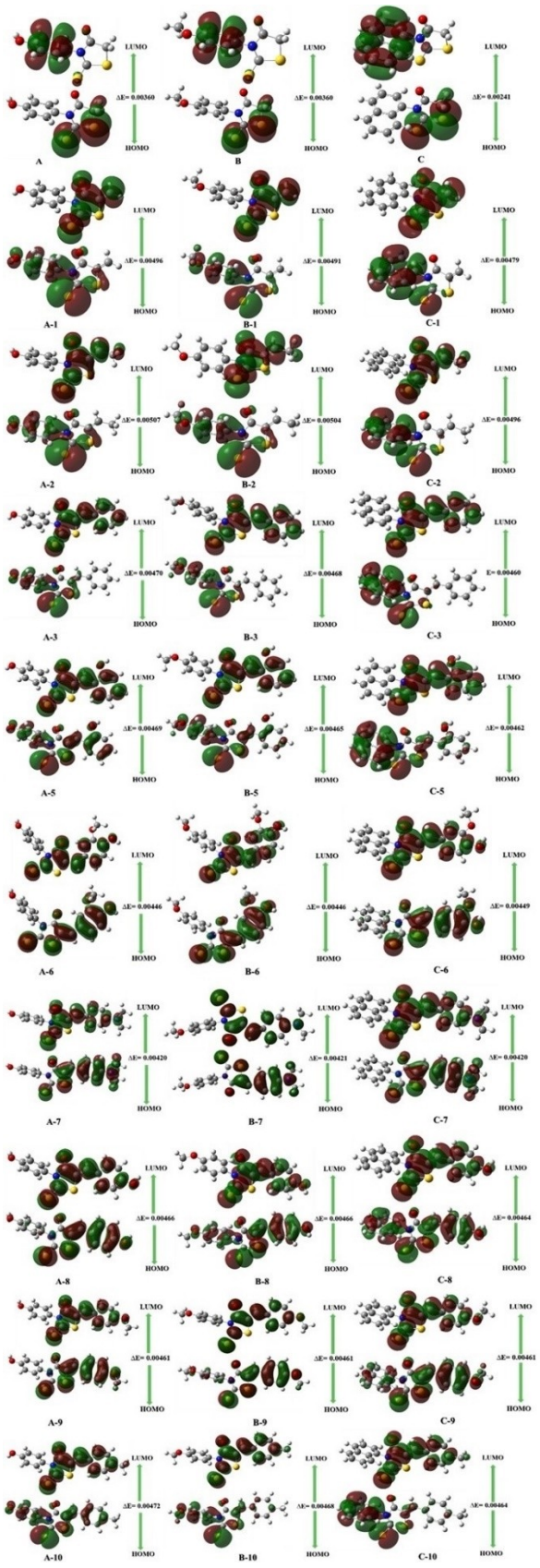

Figure 2. HOMO and LUMO representation of Compounds series **A**, **B** and **C**.

that demonstrates the interactions of very large molecules such as protein, enzymes with smaller molecules such as ligand for the discovery of new and novel drugs.[43,51] Docking studies were performed on all the 55 compounds using Molecular Operating Environment (MOE). Crystal structures of BChE, AChE, Glycoprotein SARS-Cov2, and α-glucosidase having the PDB code of 4BDS, 1EVE, 6VXX and 2Q85 respectively used for molecular docking score determination were given in Table 4. For the docking purpose, first of all hydrogen atoms were added in the protein structure, then water molecules were removed from it. The 3D protonation and energy minimization step were performed using default parameters of MOE energy minimization algorithm [gradient: 0.05, Force Field: MMFF94X]. In the end, this minimized protein structure was docked against 55 compounds belonging to 5 different series of amines including; 4-aminophenol, 4-methoxybenzeneamine, Naphthylamine, *para* toluidine, and Ethylenediamine. Total 55 compounds were analyzed by docking analysis against Spike Glycoprotein retrieved from Protein Data Bank. PyRx Virtual Screening Tool was utilized for this screening analysis.[52] AutoDock Vina was used in the PyRx environment for screening on a Windows bases Operating System equipped with a CORE i5 INTEL 7th Generation Processor and AMD Radeon Graphics Processing Unit. The PDB files of compounds were prepared by energy minimization in PyRx and screening was done against retrieved PDB file of the Spike Glycoprotein. After the energy minimization of the ligands, the best bindind affinity of Spike Glycoprotein SARS-Cov2 was found with compound A7 which was -8.7 kcal/mol. The second best binding affinity was observed with compound A5 which was -8.5 kcal/mol. The obtained docking complex was further validated by Discovery Studio Visualizer to confirm the presence of hydrogen bonding, hydrophobic interactions and Wan der Wall Forces in it. The Discovery Studio Visualizer suggested three hydrophobic interactions with distances of 3.75, 3.67, and 3.56 respectively. There were totally three hydrogen bonds were found there with the distance of 2.76, 3.48 and 3.65 respectively. From the predicted hydrogen bonding, only the first one was a protein donor. Figure 3 represents the structural presentations of docking complex. The Ligand interaction module of MOE and PyRx was used to observe the ligand-enzyme interactions while MOE and discovery studio visualizer was used for the analysis, view, and graphical representation of the docking results.

Acetylcholinesterase

In the case of AChE enzyme, a docking study of all the compounds was carried out (Figure 4) and their S score was calculated. It was found on the basis of these values that **B5** compound showed maximum interaction with the AChE enzyme having the S score of -12.9027 kcal/mol. For the very first series, the decreasing order of ligand enzyme interaction is **A6** > **A5** > **A1** > **A8** > **A10** > **A7** > **A3** > **A9** > **A** > **A2** > **A4** and for the second series of 4-methoxybenzeneamine, the order is **B5** > **B4** > **B6** > **B7** > **B8** > **B9** > **B1** > **B10** > **B3** > **B2** > **B**. The order of the third series based on docking score is **C6** > **C3** > **C5** > **C8** > **C2** > **C1** > **C7** > **C9** > **C10** > **C4** > **C**. The **D8** and **E8** com-

Table 4. Molecular docking scores of **A**, **B**, **C**, **D**, and **E** series compounds against α-Glucosidase, 1EVE, BChE, and SARS-Cov2.

Docking score (kcal/mol)					Docking score (kcal/mol)				
PDB Comp	AChE 1EVE	α-Glucosidase 2Q85	BChE 4BDS	Covid SARS-Cov2	PDB Comp	AChE 1EVE	α-Glucosidase 2Q85	BChE 4BDS	Covid SARS-Cov2
A	−9.8616	−10.4651	−3.8288	−6.1	B	−9.4089	−9.6489	−3.6080	−6.6
A1	−11.0342	−10.9790	−4.1174	−6.3	B1	−10.2806	−9.3785	−4.6419	−6.6
A2	−9.4788	−10.5791	−5.0916	−6.5	B2	−9.6130	−10.7238	−4.7268	−6.4
A3	−10.2108	−11.9404	−7.4276	−8.1	B3	−10.1952	−10.4317	−7.6919	−8
A4	−9.4405	−11.4668	−8.1407	−8.4	B4	−11.8063	−11.0378	−11.8123	−6.1
A5	−11.1245	−13.3680	−7.3486	−8.1	B5	−12.9027	−14.5905	−7.7565	−8
A6	−12.6728	−13.2526	−7.7363	−8.5	B6	−11.7120	−13.7558	−7.3938	−6
A7	−10.3377	−12.8612	−8.4166	−8.7	B7	−10.4840	−11.4710	−7.8359	−5.3
A8	−10.8511	−12.3068	−7.2407	−7.9	B8	−10.3633	−10.9823	−6.7436	−8
A9	−9.9035	−10.9808	−8.1118	−8.3	B9	−10.2838	−11.6716	−6.9841	−8.3
A10	−10.6607	−12.8143	−7.5933	−8.5	B10	−10.2296	−11.6176	−7.8015	−8.5
C	−9.5338	−9.4914	−4.7454	−6.7	D	−7.9471	−8.6886	−4.4428	−6.8
C1	−10.7309	−9.1053	−5.6633	−7.2	D1	−8.8604	−9.1117	−4.6711	−6.8
C2	−10.7609	−11.0101	−6.0197	−7.5	D2	−8.2461	−9.4299	−4.6681	−8
C3	−11.5058	−10.8187	−6.3557	−8.3	D3	−9.8060	−10.2411	−6.8175	−8.3
C4	−10.5809	−11.3471	−7.7377	−6.4	D4	−9.6241	−10.3379	−7.4956	−7.8
C5	−11.2874	−11.2233	−7.4393	−7.8	D5	−11.5847	−14.1575	−6.8445	−8.4
C6	−12.5122	−14.8735	−7.6221	−5.2	D6	−10.1902	−14.2753	−8.5584	−8.6
C7	−10.7113	−12.3032	−8.6971	−4.5	D7	−9.5292	−11.4683	−7.7214	−8.6
C8	−11.1467	−12.0873	−7.5735	−7	D8	−12.4249	−11.9791	−6.6595	−6.4
C9	−10.6931	−12.3681	−7.4572	−7.1	D9	−9.7838	−11.2171	−7.7944	−8.3
C10	−10.6083	−12.5190	−7.6422	−6.4	D10	−10.4985	−10.1050	−7.3026	−8.5
E	−7.9093	−7.7439	−3.0744	−5.3	E6	−11.6638	−12.1622	−6.0738	−6.9
E1	−8.4625	−8.0485	−3.3999	−5.4	E7	−9.6547	−10.5481	−7.6567	−6.9
E2	−8.5450	−9.5494	−3.6798	−5.6	E8	−11.8103	−10.2132	−4.6790	−6.9
E3	−9.0480	−9.9367	−5.7605	−5.5	E9	−10.6242	−10.6179	−5.2573	−6.9
E4	−10.0965	−9.8762	−4.8084	−6.7	E10	−9.9540	−9.7010	−6.2178	−6.8
E5	−11.3650	−10.3226	−5.4315	−6.8					

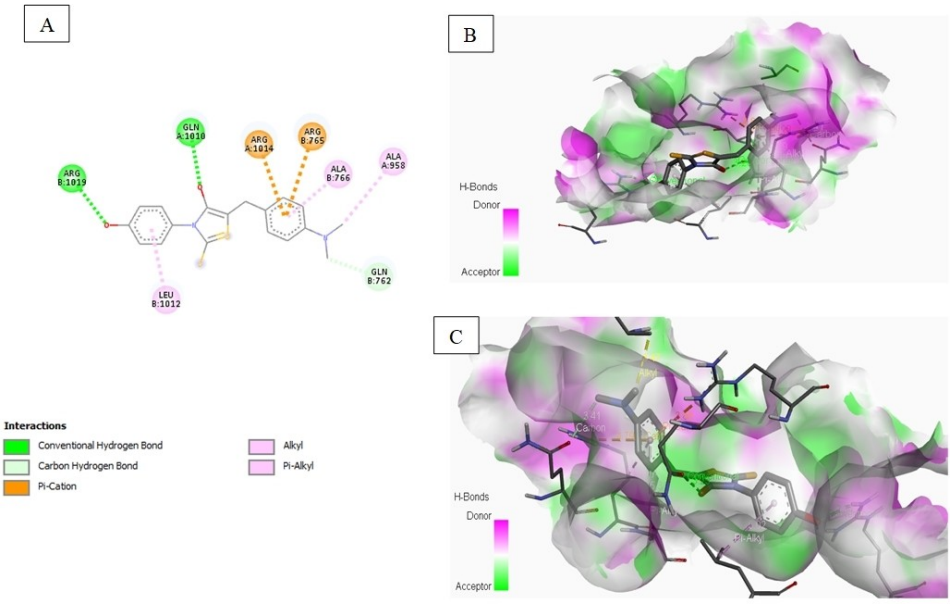

Figure 3. The best docking complex of Spike Glycoprotein & Compound A7 possessing

pounds exhibited maximum scores in their represented series while the remaining compounds give the following order **D5** > **D10** > **D6** > **D3** > **D9** > **D4** > **D7** > **D1** > **D2** > **D** and **E6** > **E5** > **E9** > **E4** > **E10** > **E7** > **E3** > **E2** > **E1** > **E**.

The compound **B5** has a maximum docking score of −12.9027 kcal/mol and also showed a number of interactions with different amino acid residues on the active site of the target acetylcholinesterase. The carbonyl oxygen and hydroxyl oxygen of the Tyr334 and Tyr70 showed hydrogen bonding

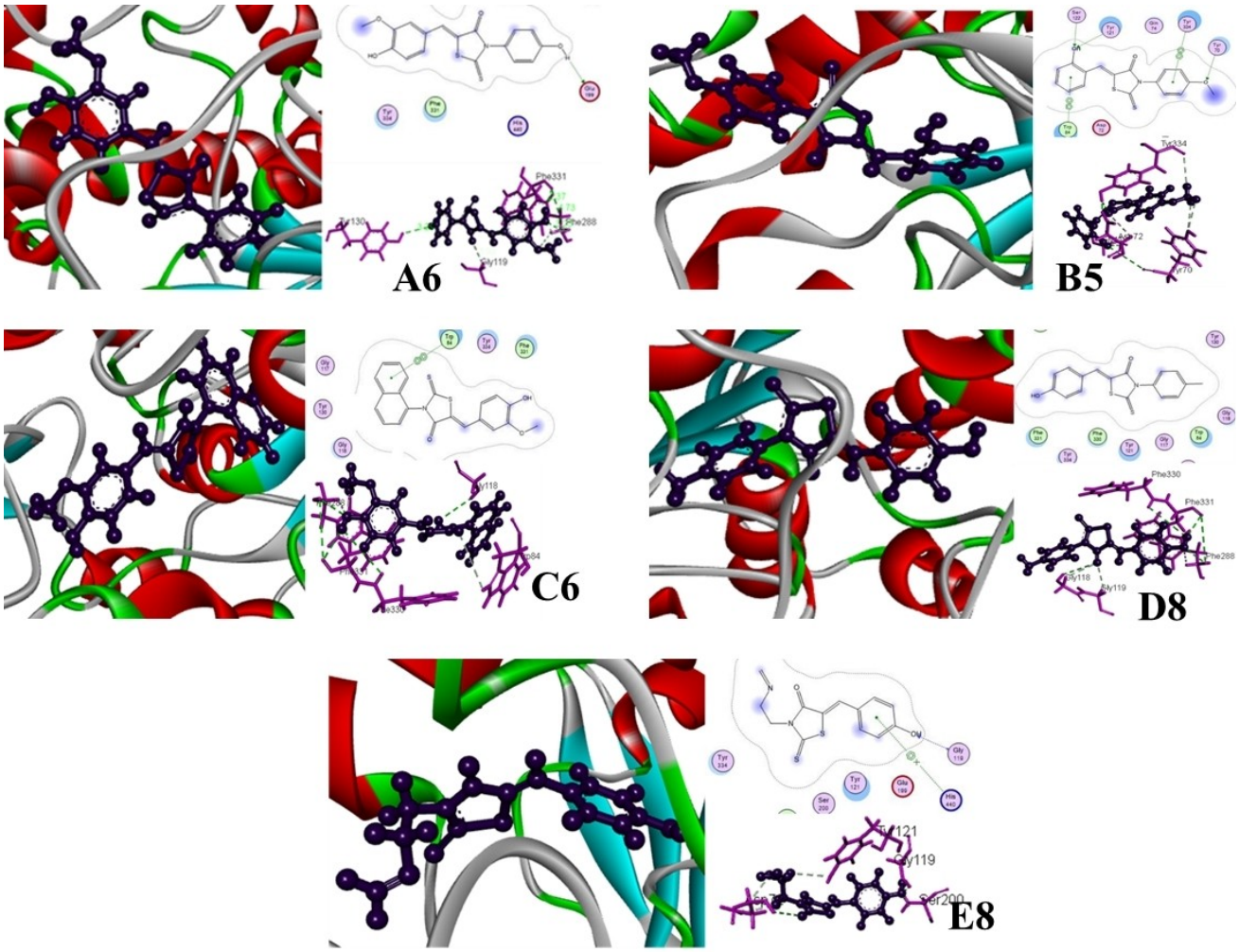

Figure 4. Different docking poses of the synthesized and proposed compounds on AChE.

with methoxy hydrogen of the compound (**B5**) at the distance of 3.43 Å and 3.29 Å respectively. Similarly, the carbonyl oxygen of Gly118 and Tyr70 demonstrated hydrogen bonding with the hydroxyl hydrogen atom. Asp72 showed hydrogen bonding with the carbonyl oxygen atom of thiazolidinone ring. The electronic cloud of Tyr334 showed pi-pi interaction with thiazolidinone ring and pi-alkyl interaction with carbon atom of the methoxy group attached as the substituent at the distance of 5.39 Å and 5.60 Å. Six membered rings of Tyr70 developed pi-pi and pi-alkyl interaction with 4-methoxyphenyl ring and with the carbon atom of the methoxy group. Metwally et al., (2019) performed the docking study and correlate it with antifungal activity. They concluded that binding energy of (−14.6964 kcal/mol) for the compound which bounds to the active sites of 1ZOY and gives the effective antifungal activity. This maximum interaction is the attribute of three hydrogen bonds between the hydroxyl group attached to the ring and the active sites of 1ZOY.[53]

In case of **A6** compound, Tyr130 showed hydrogen bonding with a hydroxyl oxygen atom. A carbonyl oxygen atom of thiazolidinone rings showed interaction with the hydrogen atom of Gly119 while Phe288 revealed interactions with hydroxyl oxygen and the carbonyl oxygen of the Phe331. Pi electronic cloud of Phe288 showed pi-pi interaction with the six-membered ring attached to the hydroxyl group at the distance of 10.34 Å. Similarly, compound **C6**, S–H, and O–H interactions are present between the sulfur, oxygen atoms of thiazolidinone ring, and hydrogen atoms of Gly118 and Trp84. The oxygen of carbonyl group of Phe330 and Phe331 exhibited hydrogen bonding with hydroxyl hydrogen at the distance of 2.80 Å and 4.61 Å respectively. The hydrogen of Phe288 revealed hydrogen bonding interaction with hydroxyl oxygen at the bond length of 3.20 Å and its six-membered electronic clouds showed pi-alkyl interaction with the sulfur atom of thiazolidinone ring. Six membered electronic cloud of Trp84, Phe330, and Phe331 developed pi-pi interaction with six-membered and five-membered rings present in the compound. The **D8** compound showed interactions with Gly118 and Gly119 due to the oxygen atom of thiazolidinone ring and hydrogen of the amino acid residue at the distance of 3.32 Å and 3.36 Å respectively. The hydrogen of the Phe288 has given hydrogen bonding with hydroxyl oxygen at the bond length of

3.64 Å and 4.65 Å. Furthermore, carbonyl oxygen of Phe330 and Phe331 showed hydrogen bonding with hydroxyl group at the distance of 4.50 Å and 2.84 Å respectively. Pi electronic cloud of Phe330 and Phe288 developed pi-pi interaction with six-membered ring of the compound at the distance of 6.90 Å and 7.24 Å. Pi-pi interaction is also shown by Phe288 with thiazolidinone ring at the distance of 8.50 Å. In the case of **E8**, the docking score was −11.8103 kcal/mol and this compound showed hydrogen interaction with Gly119 and Ser200 at the distance of 2.10 Å and 2.18 Å respectively. Sulfur hydrogen interaction is present between a sulfur atom of thiazolidinone rings and Asp72 while hydroxyl oxygen of Tyr121 revealed hydrogen bonding with the methylene hydrogen atoms attached to the ring. It also showed pi-pi interaction with the electronic cloud of thiazolidinone rings at a distance of 6.23 Å.

Butyrylcholinesterase

The synthesized, as well as proposed compounds, were also docked and their S score was calculated to estimate the interaction behavior of the ligand with the Butyrylcholinesterase. It was depicted that among all the 55 compounds, **B4** compound of 4-methoxybenzeneamine series showed a maximum score for BChE enzyme with a value of −11.8123 kcal/mol while the aminophenol series of the compounds, the highest score was shown by **A7**. The decreasing order of the **A** series compounds is **A7** > **A4** > **A9** > **A6** > **A10** > **A3** > **A5** > **A8** > **A2** > **A1** > **A** and for second series, the decreasing order is **B4** > **B7** > **B10** > **B5** > **B8** > **B3** > **B6** > **B9** > **B2** > **B1** > **B**. *N, N*-dimethyl amino benzaldehyde (**C7**) derivative of **C** showed a higher score in its respective series and the order of the compounds is **C7** > **C4** > **C10** > **C6** > **C8** > **C9** > **C5** > **C3** > **C2** > **C1** > **C**. The **D6** compound showed the maximum score among all compounds while the **D** precursor exhibited the least score toward BChE. The order of the **D** and **E** series compounds is as; **D6** > **D9** > **D7** > **D4** > **D10** > **D5** > **D3** > **D8** > **D1** > **D2** > **D** and **E7** > **E10** > **E6** > **E3** > **E5** > **E9** > **E4** > **E8** > **E2** > **E1** > **E**.

The maximum docking interaction were exhibited by **A7** compound having *N, N*-dimethyl amino substitution on the phenyl ring of the benzaldehyde and it developed interactions with Trp82 and Tyr128. Six member rings of Trp82 showed pi-pi interaction with the pi electronic cloud of the compound. It also showed pi alkyl interaction with the dimethylamino group of the compound. The hydrogen of the Typ128 developed strong interaction with the oxygen of the thiazolidinone ring at a distance of 3.38 Å. **B4** compound has shown the maximum interaction that is basically due to the presence of electron-withdrawing group present in the structure. Verma et al., (2020) reported the docking studies of series of compounds **3**–**6** (a–i) by relating to anti-TB using PDB ID 6AJG of the receptor protein. Among all the ligands, compound **5e** having Cl substituent at R_2 position forms four hydrogen bonds with the different amino acids. **5e** compound also exhibits hydrophobic interaction for H–N bond with pyrrole ring of indole moiety which indicates that 5e is the novel compound as the useful anti-TB agent.[54] Bhutani et al., (2019) elaborated the docking study to explain the binding interactions of the synthesized compounds into the active site of the PPAR-γ receptor. Three compounds Tz21, Tz17, and Tz10 exposed a maximum docking score of −9.85, −9.11, and −8.85 respectively. Tz17 is the compound having 4-methoxyphenyl moiety present in it and showed hydrogen bonding, pi-pi interaction as well as hydrophobic contact with different amino acids of peroxisome proliferator-activated receptor-gamma (PDB code: 1FM9, resolution: 2.1 A°) and alpha-glucosidase (PDB code: 2QMJ, resolution: 1.9 Å).[55] Tyr128 developed interaction with the methoxy group as well as its pi electronic cloud involved the pi alkyl interaction at the distance of 4.80 Å. It also showed interaction with the sulfur atom of thiazolidinone rings at a 5.45 Å distance. The case of **C7** carbonyl oxygen and hydroxyl oxygen of two amino acids i.e., His438 and Tyr332 revealed hydrogen bond interactions with a methyl hydrogen atom attached to the amino group of the compound. The S–H and O–H interactions were developed by Gly116 and Asp70 with oxygen, sulfur atoms present in thazolidinone ring. Tyr 332 and His438 showed pi alkyl interaction with the carbon atoms of the dimethylamino group at the distance of 6.78 Å and 8.21 Å. The compound **D6**, hydrogen bond interaction is presented between Gly115 and hydroxyl oxygen. Six membered conjugated rings of Trp82 showed interactions with five-member thiazolidinone ring via π-π interactions while an electronic cloud of Tyr332 and hydrogen atom of Asp70 revealed interactions with a sulfur atom of thiazolidinone ring. Tyr332, Asp70 and His438 developed hydrogen bonding with methyl hydrogen atoms of dimethylamine in the case of **E7**. The H….O and H….S interaction was revealed by Thr120, Ser198, and Tyr128 with oxygen and sulfur present in thiazolidinone rings respectively. Trp82 showed interaction with the nitrogen atom attached to the compound **E7**. Electronic cloud of Trp82 showed pi-pi interaction with the thiazolidinone ring and six-membered ring of the compound at 5.06 Å, 5.59 Å, 5.49 Å, and 4.35 Å distance. Trp82, His438and Tyr332 developed strong pi alkyl interaction with carbon atoms of the dimethylamino group. Docking poses of the compounds on BChE were given in Figure 5.

α-glucosidase

The α-glucosidase is the enzyme responsible for controlling sugar levels in the bloodstream. In order to check the application of the synthesized and proposed compounds against diabetes, docking studies were conducted on the active sites of the α-glucosidase illustrated in Figure 6. The docking studies revealed that **C6** compound showed a maximum docking score (−14.8735) among all the 55 compounds. Furthermore, this compound also showed strong interactions on the active site of α-glucosidase among all the series as well as the other three enzymes. On the other hand, for the aminophenol series, the maximum interaction was shown by **A5** compound, and decreasing order is **A5** > **A6** > **A7** > **A10** > **A8** > **A3** > **A4** > **A9** > **A1** > **A2** > **A**. It was observed for the second series, the decreasing score order is **B5** > **B6** > **B9** > **B10** > **B7** > **B4** > **B8** > **B2** > **B3** > **B** > **B1**. The decreasing order of the **C, D** and **E** series is **C6** > **C10** > **C9** > **C7** > **C8** > **C4** > **C5** >

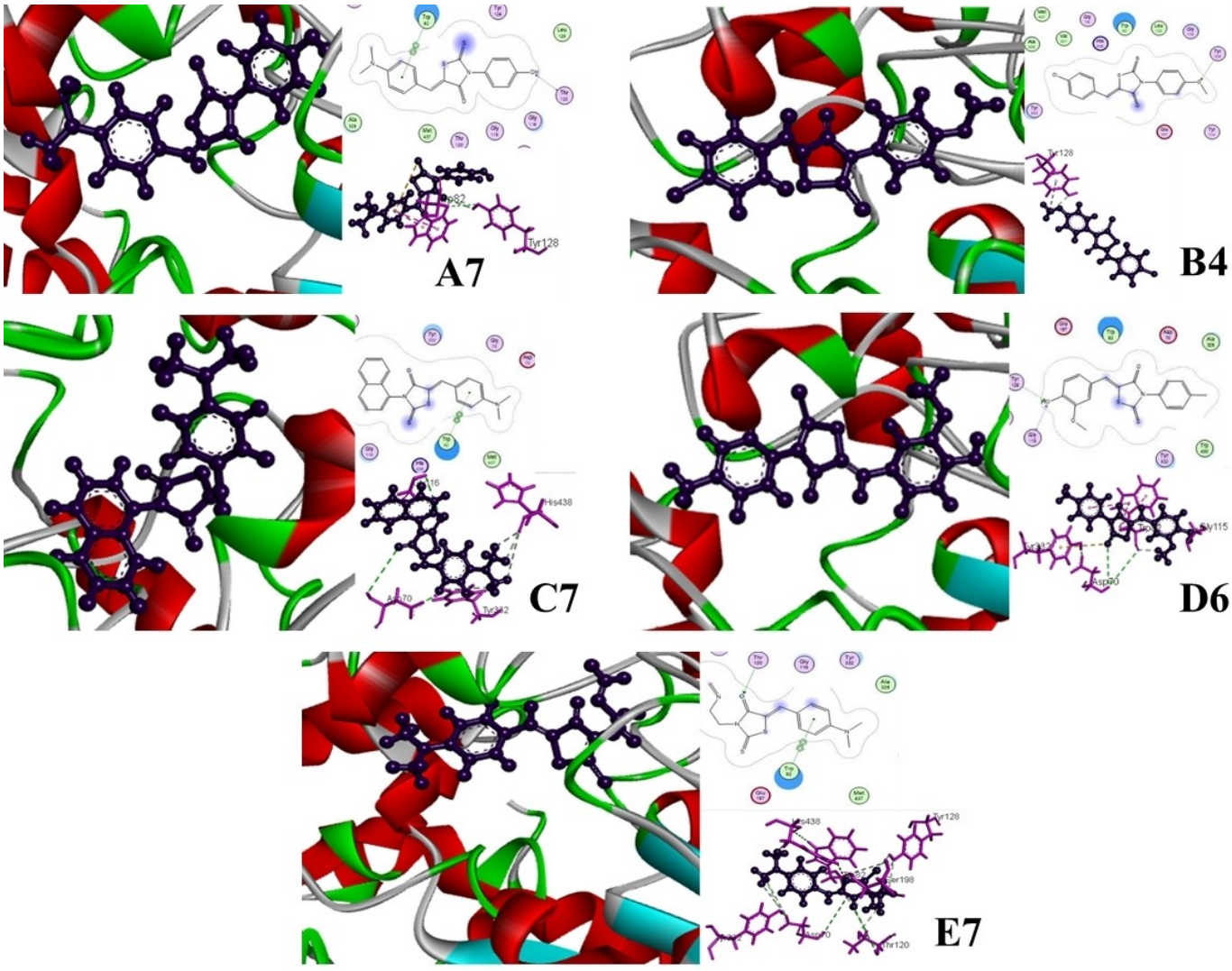

Figure 5. Different docking poses of the synthesized and proposed compounds on BChE.

C2 > **C3** > **C** > **C1**, **D6** > **D5** > **D8** > **D7** > **D9** > **D4** > **D3** > **D10** > **D2** > **D1** > **D** and **E6** > **E9** > **E7** > **E5** > **E8** > **E3** > **E4** > **E10** > **E2** > **E1** > **E** respectively.

In order to check the possible interaction of the compounds on the active sites of the enzyme, discovery studio and MOE parameters were used and it was found that for **A5** compound, both hydroxyl hydrogen atoms showed strong hydrogen bonding with the hydroxyl oxygen atom of Ser229 and Ser116 at the distance of 1.42 Å and 1.45 Å respectively. The π-electronic cloud of five and six-membered rings depicted pi donor interaction with amino hydrogen of Arg214 and Arg327. In case of **B5**, the amino hydrogen atom of Glu48 displayed hydrogen bonding with the hydroxyl oxygen atom of the compound. The amino hydrogen atom of Arg214 and Arg327 showed O–H interaction with methoxy oxygen atom of the compound and S–H interaction with Sulfur atom of thiazolidinone ring. The amino hydrogen atom of Ser50 showed hydrogen bonding with the carbonyl oxygen atom of the five-membered ring. Arg327 showed pi alkyl interaction with the six-membered ring and pi donor interaction with the thiazolidinone ring. Pi alkyl interaction is present between the electronic cloud of methoxyphenyl group and Arg214. The case of **C6** compound, Arg214, Ile110, and Pro111depicted H–O interaction with the carbonyl oxygen atom of thiazolidinone rings at the distance of 2.67 Å, 2.84 Å, and 2.33 Å respectively. The N–H of Arg327 showed hydrogen bond interaction with the methoxy oxygen atom of the compound and S–H interaction with a sulfur atom of thiazolidinone ring. Ser116 showed hydrogen bonding with a methoxy oxygen atom and alcoholic hydrogen of the compound. Six membered rings of the compounds act as the pi donor to Arg214 and Arg327 amino acids. Five and six-membered rings of the compound showed pi alkyl interaction with Arg214, Arg327, Ile110, and Pro111 at different distances. The compound **C6** depicted maximum interaction for alpha-glucosidase as well as depicted highest docking score of −14.8735, which means that compounds having a good

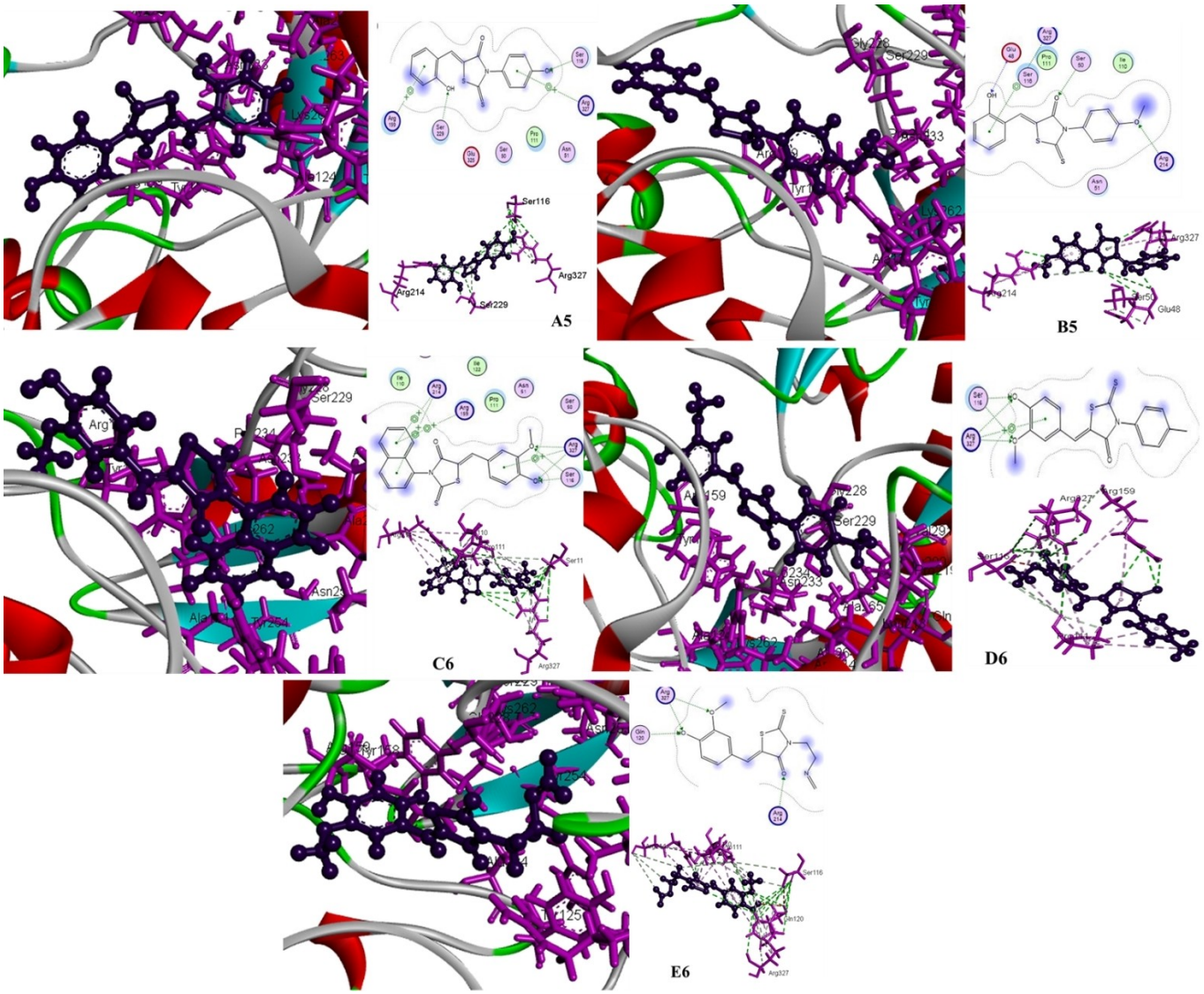

Figure 6. Different docking pose of the synthesized and proposed compounds on α-glucosidase.

score also have good interaction or binding on the active site of the enzyme. Furthermore, such compounds showed good inhibition and may be used as therapeutic agents in the near future. Salian et al., (2019) reported that compounds having $-OCH_3$ group on the benzene ring bind the active site more firmly. Similarly, this report presented that the target protein (FabH with PDB code; 5BNS) of *E. coli* has good interaction due to the presence of the methoxy group.[56] Hammad et al., (2020) reported that excellent anti-bacterial activity was revealed by the compounds having the phenyl group with the substitution of *m*-OCH3, *p*-OH, and cyclohexyl groups.[57]

In the **D6** compound, Arg159 showed S–H interaction with the sulfur atom of thiazolidinone rings while Arg327 depicted hydrogen bonding with the methoxy and hydroxy oxygen atom of the compound and pi donor interaction with the six-membered ring. Carbonyl oxygen atom of Ser116 and Pro111 hydrogen bonding with the methoxy and hydroxy hydrogen respectively. The electronic cloud of five and six-membered rings depicted pi alkyl interaction with Pro111, Arg159, and Arg327. Ser116 showed acceptor interaction with the methoxy oxygen atom of the compound. In the case of the **E6** compound, Arg214 and Ile110 interact with the carbonyl oxygen of thiazolidinone rings at the distance of 1.98 Å and 3.16 Å respectively. The carbonyl oxygen atom of Pro111 showed hydrogen bonding with methoxy hydrogen. The Arg327, amino hydrogen atom of the amino acid showed hydrogen bond interaction with the methoxy oxygen atom of the compound. Carbonyl oxygen atom of Ser116 depicted interaction with the methoxy hydrogen atom of the compound. Amino hydrogen atom and carbonyl oxygen atom showed hydrogen bonding with the hydroxyl group attached to the ring. The electronic cloud of thiazolidinone rings developed pi alkyl interaction with Arg214, Ile110, and Pro111. The electronic cloud of the six-membered ring developed pi

alkyl interaction with Arg327, Ile110, and Pro111. Gln120 showed donor interaction with the hydroxyl hydrogen atom of the compound.

Normal Mode Analysis

IModS performs structural critical analysis by altering the complex's force field with regard to different time intervals.[42] The resulting model exhibits reduced distortion at each capacity level of the leftovers. The complex's eigon value is 3.776919e−05 that represents the energy required to deform the structure. Heat maps with low RMSD and strongly co-related regions demonstrated improved relationships between individual residues.[58] The heat maps and the related figures of Normal Mode Analysis are given below in the Figure 7.

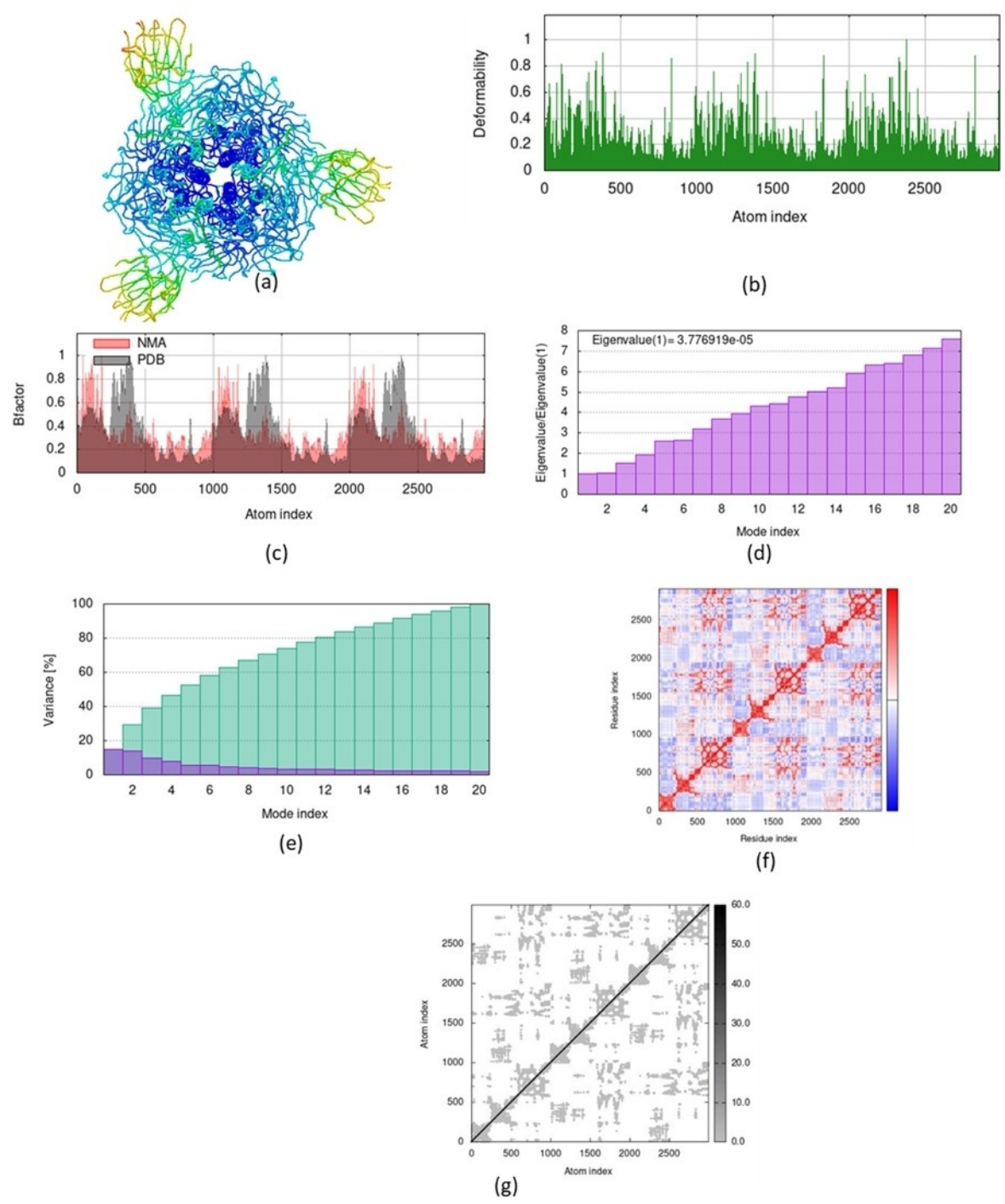

Figure 7. Normal Mode Analysis A-10 with Spike Protein Coronavirus (PDB ID: 6vxx).
(A) Simulated 3D model (B) Deformability (C) B factor (D) Eigen values (E) Variance (F) Co- variance map (G) Elastic network

Admet Study

ADMET properties of under consideration compounds were determined by Swiss online-based software. Parameters that were mostly discussed; molecular weight, topological surface area (TPSA), Gastral intestinal absorption, the BBB permeant, *P*-glycoprotein substrates and inhibitors, and skin permeation arranged in Tables 5–9. Lipinski's 5.0 rule differentiates between drug-like or non-drug-like molecules. The range of molecular weight in the **A**, **B**, **C**, **D**, and **E** series was (225.29–359.46), (239.31–371.43), (259.35–393.48), (223.31–357.45), and (188.27–322.40) respectively. Compound **C7** had the highest molecular weight (393.48) while compound **E** lowest molecular weight value of 188.27. The molecular weight (MW) of all compounds was below 500 Dalton to permit skin absorption and act as drug-like candidates.[59] Topological Polar surface area (TPSA) of **A**, **B**, **C**, **D**, and **E** series was seen in a range between (97.93–118.16), (86.93–124.23), (77.70–107.16), (77.70–107.16), and (90.06–119.52) respectively. Different substituents contributed differently to the TPSA ($Å^2$) values as NR_3 (3.24), R–O–R (9.23), R–O–H (20.23), C=O (17.07), S=R (32.09), R–S–R (25.30), OH–R (23.06), where R was a non-hydrogen atom.[60]

Table 5. *In-Silico* ADMET study of **A** serie compounds.

Properties	Compounds										
	A	A1	A2	A3	A4	A5	A6	A7	A8	A9	A10
Physiochemical											
Molecular weight	225.29	230	251.32	313.39	347.84	329.39	3.59.42	356.46	329.39	343.42	327.42
No of heavy atoms	14	15	16	21	22	22	24	24	22	23	22
Fraction Csp^3	0.11	0.00	0.09	0.00	0.00	0.00	0.06	0.11	0.00	0.06	0.06
Num. H-bond acceptors	2	2	1	2	2	3	4	2	3	3	2
TPSA ($Å^2$)	97.93	97.93	97.93	97.93	97.93	118.16	127.39	101.17	118.16	107.16	97.93
Consensus Log $P_{o/w}$	1.67	2.07	2.34	3.32	3.86	2.89	2.93	3.30	2.89	3.29	3.64
Log S (ESOL)	−2.79	−3.24	−3.45	−4.71	−5.30	−4.57	−4.63	−4.93	−4.57	−4.77	−5.01
Pharmacokinetics											
GI absorption	High	High	High	High	High	High	High	High	High	High	High
BBB Permeant	No	No	No	No	No	No	No	No	No	No	No
P-gp substrate	No	No	No	No	No	No	No	No	No	No	No
Drug Likeness & Medicinal chemistry											
Lipinski	Yes; 0 violation	Yes; 0 violation	Yes; 0 violation	Yes; 0 violation	Yes; 0 violation	Yes; 0 violation	Yes; 0 violation	Yes; 0 violation	Yes; 0 violation	Yes; 0 violation	Yes; 0 violation
Veber	Yes	Yes	Yes	Yes	Yes	Yes	Yes	Yes	Yes	Yes	Yes
PAINS	1 alert	1 alert	1 alert	1 alert	1 alert	1 alert	1 alert	2 alerts	1 alert	1 alert	1 alert
Synthetic accessibility	2.23	2.45	2.72	3.01	2.99	3.13	3.18	3.28	3.04	3.09	3.12

Table 6. *In-Silico* ADMET study of **B** serie compounds.

Properties	Compounds										
	B	B1	B2	B3	B4	B5	B6	B7	B8	B9	B10
Physiochemical											
Molecular weight	239.31	251.32	265.35	327.42	3.61.87	343.42	3.71.43	370.49	343.42	357.45	341.45
No of heavy atoms	15	16	17	22	23	23	25	25	23	24	23
Fraction Csp^3	0.20	0.09	0.17	0.06	0.06	0.06	0.06	0.16	0.06	0.11	0.11
Num. H-bond acceptors	2	2	2	2	2	3	4	2	3	3	2
TPSA ($Å^2$)	86.93	86.93	86.93	86.93	86.93	107.16	124.23	90.17	107.16	96.16	86.93
Consensus Log $P_{o/w}$	2.08	2.48	2.74	3.72	4.25	3.30	3.07	3.73	3.31	3.71	4.06
Log S (ESOL)	−2.99	−3.44	−3.66	−4.92	−6.70	−4.77	−4.51	−5.15	−4.77	−4.98	−5.21
Pharmacokinetics											
GI absorption	High	High	High	High	High	High	High	High	High	High	High
BBB Permeant	No	No	No	No	No	No	No	No	No	No	No
P-gp substrate	No	No	No	No	No	No	No	No	No	No	No
Drug Likeness & Medicinal chemistry											
Lipinski rule	Yes; 0 violation	Yes; 0 violation	Yes; 0 violation	Yes; 0 violation	Yes; 0 violation	Yes; 0 violation	Yes; 0 violation	Yes; 0 violation	Yes; 0 violation	Yes; 0 violation	Yes; 0 violation
Veber rule	Yes	Yes	Yes	Yes	Yes	Yes	Yes	Yes	Yes	Yes	Yes
PAINS	1 alert	1 alert	1 alert	1 alert	1 alert	1 alert	1 alert	2 alerts	1 alert	1 alert	1 alert
Synthetic accessibility	2.26	2.49	2.75	3.06	3.04	3.17	3.18	3.33	3.09	3.19	3.17

Table 7. *In-Silico* ADMET study of **C** serie compounds.

Properties	Compounds										
	C	C1	C2	C3	C4	C5	C6	C7	C8	C9	C10
Physiochemical											
Molecular weight	259.35	271.36	285.38	347.45	381.90	363.45	393.48	390.52	363.45	377.48	361.48
No of heavy atoms	17	18	19	24	25	25	27	27	25	26	25
Fraction Csp^3	0.08	0.00	0.07	0.00	0.00	0.00	0.05	0.09	0.00	0.05	0.05
Num. H-bond acceptors	1	1	1	1	1	2	1	1	2	2	1
TPSA (Å^2)	77.70	77.70	77.70	77.70	77.70	97.93	107.16	80.94	97.93	86.93	77.70
Consensus Log $P_{o/w}$	3.02	3.41	3.67	4.61	5.16	4.17	4.23	4.59	4.17	4.60	4.96
Log S (ESOL)	−4.12	−4.57	−4.78	−6.00	−6.59	−5.86	−5.92	−6.23	−5.86	−6.07	−6.30
Pharmacokinetics											
GI absorption	High	High	High	High	High	High	High	High	High	High	High
BBB Permeant	Yes	Yes	Yes	No	No	No	No	No	No	No	No
P-gp substrate	No	No	No	No	No	No	No	No	No	No	No
Drug Likeness & Medicinal chemistry											
Lipinski rule	Yes; 0 violation	Yes; 0 violation	Yes; 0 violation	Yes; 0 violation	Yes; 0 violation	Yes; 0 violation	Yes; 0 violation	Yes; 0 violation	Yes; 0 violation	Yes; 0 violation	Yes; 0 violation
Veber rule	Yes	Yes	Yes	Yes	Yes	Yes	Yes	Yes	Yes	Yes	Yes
PAINS	1 alert	1 alert	1 alert	1 alert	1 alert	1 alert	1 alert	2 alerts	1 alert	1 alert	1 alert
Synthetic accessibility	2.47	2.69	2.96	3.26	3.23	3.29	3.35	3.53	3.21	3.26	3.36

Table 8. *In-Silico* ADMET study of **D** serie compounds.

Properties	Compounds										
	D	D1	D2	D3	D4	D5	D6	D7	D8	D9	D10
Physiochemical											
Molecular weight	223.31	235.33	249.35	311.42	345.87	327.42	357.45	354.49	327.42	341.45	249.35
No of heavy atoms	14	15	16	21	22	22	24	24	22	23	16
Fraction Csp^3	0.20	0.09	0.17	0.06	0.06	0.06	0.11	0.16	0.06	0.11	0.17
Num. H-bond acceptors	1	1	1	1	1	2	3	1	2	2	1
TPSA (Å^2)	77.70	77.70	77.70	77.70	77.70	97.93	107.16	80.94	97.93	86.93	77.70
Consensus Log $P_{o/w}$	2.44	2.83	3.10	4.07	4.59	3.69	3.69	4.07	3.64	4.05	3.10
Log S (ESOL)	−3.23	−3.68	−3.89	−5.15	−5.74	−5.01	−5.08	−5.37	−5.01	−5.21	−3.89
Pharmacokinetics											
GI absorption	High	High	High	High	High	High	High	High	High	High	High
BBB Permeant	No	Yes	Yes	No	No	No	No	No	No	No	Yes
P-gp substrate	No	No	No	No	No	No	No	No	No	No	No
Drug Likeness & Medicinal chemistry											
Lipinski rule	Yes; 0 violation	Yes; 0 violation	Yes; 0 violation	Yes; 0 violation	Yes; 0 violation	Yes; 0 violation	Yes; 0 violation	Yes; 0 violation	Yes; 0 violation	Yes; 0 violation	Yes; 0 violation
Veber rule	Yes	Yes	Yes	Yes	Yes	Yes	Yes	Yes	Yes	Yes	Yes
PAINS	1 alert	1 alert	1 alert	1 alert	1 alert	1 alert	1 alert	2 alerts	1 alert	1 alert	1 alert
Synthetic accessibility	2.23	2.47	2.74	3.14	3.12	3.18	3.24	3.42	3.09	3.15	2.74

Gastrointestinal absorption was seen high in all series of compounds. There was also no blood-brain barrier permeation was seen in all compounds except in **C**, **C1**, **C2**, **D1**, **D2**. BBB crossing drugs can cause more risk of side effects.[61] All compounds followed the Lipinski Rule (molecular mass lower than 500 Dalton, the value of Log $P_{o/w}$ did not exceed 5, hydrogen bond donor groups no more than 5, and hydrogen bond acceptors also no more than 10). Compounds exhibited effective values of synthetic accessibility for **A** (2.23–3.28), **B** (2.26–3.33), **C** (2.47–3.53), **D** (2.23–3.24), and **E** (2.71–3.29). Compound **C7** exhibited the highest synthetic accessibility value of 3.53. The structure-activity relationship (SAR) also affects the parameters of ADMET. In the case of Compound **A**, **B**, **C**, **D**, and **E** lipid permeability values varies as 1.67, 2.08, 3.02, 2.4, and 1.17 respectively. As the molecular weight of compounds increased the solubility of compounds were decreased.[61]

The order of solubility of compounds was also dependent upon various substitutions on aniline rings **C**:−4.12, **D**:−3.23, **B**: −2.99, **A**:−2.79, **E**: −2.06. The promising water and lipid solubility of a drug-affected its pathway of adsorption, distribution, metabolism, durability of action, and elimination.

Table 9. *In-Silico* ADMET study of **E** serie compounds.

Properties	Compounds										
	E	E1	E2	E3	E4	E5	E6	E7	E8	E9	E10
Physiochemical											
Molecular weight	188.27	200.28	214.31	276.38	310.82	292.38	322.40	319.44	292.38	306.40	290.40
No of heavy atoms	11	12	13	18	19	19	21	21	19	20	19
Fraction Csp^3	0.50	0.29	0.38	0.15	0.15	0.15	0.21	0.27	0.15	0.21	0.21
Num. H-bond acceptors	2	2	2	2	2	3	4	2	3	3	2
TPSA (Å^2)	90.06	90.06	90.06	90.06	90.06	110.29	119.52	93.30	110.29	99.29	90.06
Consensus Log $P_{o/w}$	1.17	1.58	1.87	2.89	3.44	2.48	2.53	2.91	2.48	2.89	3.23
Log S (ESOL)		−2.53	−2.77	−4.13	−4.72	−3.98	−4.06	−4.37	−3.98	−4.20	−4.43
Pharmacokinetics											
GI absorption	High	High	High	High	High	High	High	High	High	High	High
BBB Permeant	No	No	No	No	No	No	No	No	No	No	No
P-gp substrate	No	No	No	No	No	No	No	No	No	No	No
Drug Likeness & Medicinal chemistry											
Lipinski rule	Yes; 0 violation	Yes; 0 violation	Yes; 0 violation	Yes; 0 violation	Yes; 0 violation	Yes; 0 violation	Yes; 0 violation	Yes; 0 violation	Yes; 0 violation	Yes; 0 violation	Yes; 0 violation
Veber rule	Yes	Yes	Yes	Yes	Yes	Yes	Yes	Yes	Yes	Yes	Yes
PAINS	1 alert	1 alert	1 alert	1 alert	1 alert	1 alert	1 alert	2 alerts	1 alert	1 alert	1 alert
Synthetic accessibility	2.71	2.89	3.10	3.16	3.13	3.21	3.24	3.29	3.12	3.16	3.26

On average solubility of a drug was a composite sum of each functionality present in it. Hydrophilic functional groups had been capable to ionize and forming hydrogen bonds. Functionalities that were contributed towards water solubility of compounds: Ar–OH, $N(CH3)_2$, A-NH_2, and N=CH_2 however, those that were unable to ionize or formed hydrogen bonds tend to impart a measure of lipid solubility to a drug molecule. The main lipid-soluble functional groups were the Aromatic ring and ring system like in **C**, C=C, aliphatic alkyl chain, R–O–R, halogen group (Cl).[62] Pan Assay interference structures were able to react nonspecifically with various biological targets than specific ones because of the presence of disruptive functional groups in PAINS. In (PAINS), compounds **A7**, **B7**, **C7**, **D7**, **E7** give 2 alerts that were due to Rhodanines (ene_rhod_A) and (anil_di_alk_B) group while in case of all other compounds only exhibits single alert owing to the presence of only Rhodanines (ene_rhod_A).[63]

Conclusion

World Health Organization declared coronavirus-2019 as a pandemic disease that causes severe acute respiratory syndrome and enters the central nervous system (CNS) by distributing in the blood-brain barrier (BBB). Thiazolidinone derivatives have greater biological activities in the recent era such as antimicrobial, antioxidants, analgesic, peroxisome proliferator activator gamma receptor (PPAR), antitumor, cystic fibrosis trans-membrane conductance regulator (CFTR), anti-diabetics, anti-inflammatory, and agonist for follicle-stimulating hormone (FSH). Keeping in view the importance of COVID-19 toward the health problems of human beings, the present project was designed to check the potential of synthesized and proposed thiazolidinones against COVID-19, Alzheimer and Diabetic using molecular models. The precursors (**A**–**C**) were proposed via three steps method which further reacts with various aldehydes to convert into their respective compounds. With the help of Gaussian 09, we performed the quantum chemical calculation, and results were seen with the help of Gauss View 5.0. The 6-31G (d, p) basis set and hybrid functional B3LYP method were used to optimize the geometry of the compound and for the calculation of different parameters. The energy gap of compounds between HOMO was arranged from 0.09812–0.13516 and maximum ΔE was exhibited by **C2** while compound **A** has the least energy gap. Docking studies were performed on all 55 compounds. The compounds **C6** showed a maximum docking score (−14.8735 kcal/mol) for the alpha-glucosidase enzyme using PDB file 2Q85. AutoDock Vina was used for the docking analysis of SARS-Cov2 in the PyRx environment for screening on a Windows bases Operating System. Compounds were analyzed against Spike Glycoprotein by using PDB ID of 6VXX. The Discovery Studio Visualizer exhibited hydrogen bonding and hydrophobic and interactions. ADMET properties of under consideration compounds were determined by Swiss online-based software according to which almost all compounds followed the Lipinski rule, give high Gastrointestinal absorption and effective values of synthetic accessibility.

Data and Software Availability

We used the MOE for molecular docking and Gaussian 09 for DFT studies.

Acknowledgements

The authors are grateful to Dr. Umer Rashid, COMSATS University, Islamabad, Pakistan for helping in molecular docking studies on MOE.

Conflict of Interest

The authors declare no conflict of interest.

Keywords: COVID-19 · DFT · *In silico* studies · Molecular Docking · Thiazolidinone

[1] T. Dalmay, *Annual plant reviews. Plant Epigenetics* **2007**, *19*, 223–243.
[2] D. D. Richman, R. J. Whitley, F. G. Hayden, *Clinical Virology*, John Wiley & Sons, **2020**.
[3] D. Kumar, K. Kumari, V. K. Vishvakarma, A. Jayaraj, D. Kumar, V. K. Ramappa, R. Patel, V. Kumar, S. K. Dass, R. Chandra, *J. Biomol. Struct. Dyn.* **2020**, 1–15.
[4] S. F. Ahmed, A. A. Quadeer, M. R. McKay, *Viruses* **2020**, *12*, 254.
[5] C. Wang, P. W. Horby, F. G. Hayden, G. F. Gao, *The Lancet* **2020**, *395*, 470–473.
[6] T. Singhal, *Indian J. Pediatr.* **2020**, *87*, 281–286.
[7] L. Duan, G. Zhu, *The Lancet Psychiatry* **2020**, *7*, 300–302.
[8] D.-G. Ahn, H.-J. Shin, M.-H. Kim, S. Lee, H.-S. Kim, J. Myoung, B.-T. Kim, S.-J. Kim, *J. Microbiol. Biotechnol.* **2020**, *30*, 313–324.
[9] C. Rothe, M. Schunk, P. Sothmann, G. Bretzel, G. Froeschl, C. Wallrauch, T. Zimmer, V. Thiel, C. Janke, W. Guggemos, *N. Engl. J. Med.* **2020**, *382*, 970–971.
[10] a) M. Ciaccio, B. Lo Sasso, C. Scazzone, C. M. Gambino, A. M. Ciaccio, G. Bivona, T. Piccoli, R. V. Giglio, L. Agnello, *Brain Sci.* **2021**, *11*, 305.
[11] E. R. Hascup, K. N. Hascup, *Gerosci.* **2020**, *42*, 1083–1087.
[12] E. E. Brown, S. Kumar, T. K. Rajji, B. G. Pollock, B. H. Mulsant, *Am. J. Geriatr. Psychiatry* **2020**, *28*, 712–721.
[13] J. Schofield, L. Leelarathna, H. Thabit, *Diabetes Ther.* **2020**, *11*, 1429–1435.
[14] A. Sinclair, K. Dhatariya, O. Burr, D. Nagi, K. Higgins, D. Hopkins, M. Patel, P. Kar, C. Gooday, D. Howarth, *Diabetic Med.* **2020**, *37*, 1090–1093.
[15] P. Accounts, Coronavirus (COVID-19) Information, **2020**.
[16] L. Zou, F. Ruan, M. Huang, L. Liang, H. Huang, Z. Hong, J. Yu, M. Kang, Y. Song, J. Xia, *N. Engl. J. Med.* **2020**, *382*, 1177–1179.
[17] N. Chen, M. Zhou, X. Dong, J. Qu, F. Gong, Y. Han, Y. Qiu, J. Wang, Y. Liu, Y. Wei, *The Lancet* **2020**, *395*, 507–513.
[18] J. A. Balogun, *Afr. J. Reprod. Health* **2020**, *24*, 14–21.
[19] W. E. Villamil-Gómez, O. González-Camargo, J. Rodriguez-Ayubi, D. Zapata-Serpa, A. J. Rodriguez-Morales, *J. Infect. Public Health* **2016**, *9*, 684–686.
[20] B. Berkhout, F. van Hemert, *Virus Res.* **2015**, *202*, 41–47.
[21] P. Martins, J. Jesus, S. Santos, L. R. Raposo, C. Roma-Rodrigues, P. V. Baptista, A. R. Fernandes, *Molecules* **2015**, *20*, 16852–16891.
[22] E. Vitaku, D. T. Smith, J. T. Njardarson, *J. Med. Chem.* **2014**, *57*, 10257–10274.
[23] S. Cascioferro, B. Parrino, D. Carbone, D. Schillaci, E. Giovannetti, G. Cirrincione, P. Diana, *J. Med. Chem.* **2020**, *63*, 7923–7956.
[24] A. C. Tripathi, S. J. Gupta, G. N. Fatima, P. K. Sonar, A. Verma, S. K. Saraf, *Eur. J. Med. Chem.* **2014**, *72*, 52–77.
[25] M. J. Pucci, J. J. Bronson, J. F. Barrett, K. L. DenBleyker, L. F. Discotto, J. C. Fung-Tomc, Y. Ueda, *Antimicrob. Agents Chemother.* **2004**, *48*, 3697–3701.
[26] N. Hosseinzadeh, S. Seraj, M. E. Bakhshi-Dezffoli, M. Hasani, M. Khoshneviszadeh, S. Fallah-Bonekohal, M. Abdollahi, A. Foroumadi, A. Shafiee, *Iran. J. Pharm. Res.* **2013**, *12*, 325.
[27] A. Jain, A. Vaidya, V. Ravichandran, *Bioorg. Med. Chem.* **2012**, *20*, 3378–3395.
[28] B. Shah, P. Modi, S. R. Sagar, *Life Sci.* **2020**, *252*, 117652.
[29] I. A. Guedes, C. S. de Magalhães, L. E. Dardenne, *Biophys. Rev. Lett.* **2014**, *6*, 75–87.
[30] D. Shahwar, M. N. Tahir, M. A. Raza, B. Iqbal, S. Naz, *Acta Crystallogr. Sect. E* **2009**, *65*, o2637-o2637.
[31] D. Shahwar, M. N. Tahir, M. A. Raza, B. Iqbal, *Acta Crystallogr. Sect. E* **2009**, *65*, o2903-o2903.
[32] D. Shahwar, M. N. Tahir, N. Ahmad, M. A. Raza, S. Aslam, *Acta Crystallogr. Sect. E* **2010**, *66*, o2159-o2159.
[33] Aisha, M. A. Raza, S. H. Sumrra, K. Javed, Z. Saqib, J. K. Maurin, A. Budzianowski, *J. Mol. Struct.* **2020**, *1219*, 128609.
[34] M. Frisch, G. Trucks, H. Schlegel, G. Scuseria, M. Robb, J. Cheeseman, G. Scalmani, V. Barone, B. Mennucci, G. Petersson, *Wallingford Ct* **2009**.
[35] C. Lee, W. Yang, R. G. Parr, *Physical Rev. B* **1988**, *37*, 785.
[36] P. C. Hariharan, J. A. Pople, *Theor. Chim. Acta* **1973**, *28*, 213–222.
[37] A. Ilyas, N. Muhammad, M. A. Gilani, K. Ayub, I. F. Vankelecom, A. L. Khan, *J. Membr. Sci.* **2017**, *543*, 301–309.
[38] S. Sherzaman, M. N. Ahmed, B. A. Khan, T. Mahmood, K. Ayub, M. N. Tahir, *J. Mol. Struct.* **2017**, *1148*, 388–396.
[39] C. S. Reddy, G. R. Kumar, M. V. Devi, A. Nagaraj, *Acta Chim. Slov.* **2011**, *58*, 576–581.
[40] M. Danish, A. Bibi, M. A. Raza, N. Noreen, M. N. Arshad, M. A. Aisri, *Acta Chim. Slov.* **2020**, *67*, 785–798.
[41] T. E. Tallei, S. G. Tumilaar, N. J. Niode, B. J. Kepel, R. Idroes, Y. Effendi, S. A. Sakib, T. B. Emran, *Scientifica* **2020**, *2020*.
[42] J. R. López-Blanco, J. I. Aliaga, E. S. Quintana-Ortí, P. J. N. A. R. Chacón, **2014**, *42*, W271–W276.
[43] M. A. Raza, K. Fatima, *J. Phys. Org. Chem.* **2020**, *33*, e4076.
[44] N. Dege, M. A. Raza, O. E. Doğan, T. Ağar, M. W. Mumtaz, *J. Iran. Chem. Soc.* **2021**, 1–24.
[45] K. Schwarz, *J. Solid State Chem.* **2003**, *176*, 319–328.
[46] Y. Megrouss, F. T. Baara, N. Boukabcha, A. Chouaih, A. Hatzidimitriou, A. Djafri, F. Hamzaoui, *Acta Chim. Slov.* **2019**, *66*, 490–500.
[47] N. E. H. Belkafouf, F. T. Baara, A. Altomare, R. Rizzi, A. Chouaih, A. Djafri, F. Hamzaoui, *J. Mol. Struct.* **2019**, *1189*, 8–20.
[48] M. Soltani, H. R. Memarian, H. Sabzyan, *J. Mol. Struct.* **2018**, *1173*, 903–917.
[49] S. El-Taher, M. Metwaly, *J. Mol. Struct.* **2017**, *1134*, 840–850.
[50] M. A. Raza, S. H. Sumrra, K. Javed, Z. Saqib, J. K. Maurin, A. Budzianowski, *J. Mol. Struct.* **2020**, *1219*, 128609.
[51] K. K. Chaudhary, N. Mishra, *Database* **2016**, *3*.
[52] S. Dallakyan, A. J. Olson, in *Chemical Biology*, Springer, **2015**, 243–250.
[53] N. H. Metwally, I. T. Radwan, W. S. El-Serwy, M. A. Mohamed, *Bioorg. Chem.* **2019**, *84*, 456–467.
[54] V. A. Verma, A. R. Saundane, R. S. Meti, R. Shamrao, V. Katkar, *Polycyclic Aromat. Compd.* **2020**, 1–15.
[55] R. Bhutani, D. P. Pathak, G. Kapoor, A. Husain, M. A. Iqbal, *Bioorg. Chem.* **2019**, *83*, 6–19.
[56] V. V. Salian, B. Narayana, B. K. Sarojini, M. S. Kumar, K. S. Chandra, A. G. Lobo, *J. Mol. Struct.* **2019**, *1192*, 91–104.
[57] S. G. Hammad, M. G. El-Gazzar, N. S. Abutaleb, D. Li, I. Ramming, A. Shekhar, M. Abdel-Halim, E. Z. Elrazaz, M. N. Seleem, U. Bilitewski, *Bioorg. Chem.* **2020**, *95*, 103517.
[58] J. A. Kovacs, P. Chacón, R. J. P. S. Abagyan, *Function, Bioinformatics* **2004**, *56*, 661–668.
[59] P. Schnider, Overview of Strategies for Solving ADMET Challenges, **2021**.
[60] P. Ertl, B. Rohde, P. Selzer, *J. Med. Chem.* **2000**, *43*, 3714–3717.
[61] X. Bao, J. Wu, Y. Xie, S. Kim, S. Michelhaugh, J. Jiang, S. Mittal, N. Sanai, J. Li, *Clin. Pharmacol. Ther.* **2020**, *107*, 1116–1127.
[62] P. Gleeson, G. Bravi, S. Modi, D. Lowe, *Bioorg. Med. Chem.* **2009**, *17*, 5906–5919.
[63] J. B. Baell, G. A. Holloway, *J. Med. Chem.* **2010**, *53*, 2719–2740.

Submitted: May 7, 2022
Accepted: August 24, 2022